

Color-singlet J/ψ production at $\mathcal{O}(\alpha_s^6)$ in Υ decayZhi-Guo He^{1,2} and Jian-Xiong Wang¹¹*Institute of High Energy Physics, Chinese Academy of Science, P.O. Box 918(4), Beijing, 100049, China and Theoretical Physics Center for Science Facilities, (CAS) Beijing, 100049, China*²*Departament d'Estructura i Constituents de la Matèria and Institut de Ciències del Cosmos, Universitat de Barcelona Diagonal, 647, E-08028 Barcelona, Catalonia, Spain*

(Received 9 September 2010; published 30 November 2010)

To clarify the conflict between the theoretical predictions and experimental measurements of the inclusive J/ψ production in Υ decay, we consider the α_s^6 order color-singlet (CS) contributions of processes $\Upsilon \rightarrow J/\psi + gg$ and $\Upsilon \rightarrow J/\psi + gggg$. Both the branching ratio and the J/ψ momentum spectrum are calculated, and the branching ratio (4.7×10^{-4}) is larger than the leading-order contribution (α_s^5 , $\Upsilon \rightarrow J/\psi + c\bar{c}g$). Together with the QCD and QED leading-order contributions considered in our previous work, the CS prediction of the branching ratio for the direct J/ψ production is $\text{Br}(\Upsilon \rightarrow J/\psi_{\text{direct}} + X) = 0.90^{+0.49}_{-0.31} \times 10^{-4}$, which is still about 3.8 times less than the CLEO measurement. We also obtain a preliminary CS prediction of $R_{cc} = \frac{\mathcal{B}(\Upsilon \rightarrow J/\psi + c\bar{c} + X)}{\mathcal{B}(\Upsilon \rightarrow J/\psi + X)}$ and find that the value $0.39^{+0.21}_{-0.20}$ is much larger than the color-octet prediction, and suggest to measure this quantity in future experimental analysis.

DOI: 10.1103/PhysRevD.82.094033

PACS numbers: 12.38.Bx, 13.25.Gv, 14.40.Pq

The existence of a hierarchy of energy scales: $m_Q \gg m_Q v \gg m_Q v^2$ makes the heavy quarkonium system an ideal laboratory to study both perturbative and nonperturbative aspects of QCD, where v , being assumed to be much smaller than 1, is the velocity of a heavy quark in the rest frame of the heavy meson. And it is commonly believed that the nonrelativistic QCD (NRQCD) [1] effective theory provides a rigorous factorization formula to separate the physics in different scales. The NRQCD not only covers the results of previous color-singlet (CS) model predictions, in which at short distance the $Q\bar{Q}$ can only be in the color-singlet configuration with the same quantum numbers as the corresponding heavy quarkonium state, it also includes the contribution of $Q\bar{Q}$ in the color-octet (CO) configuration at short distance.

Despite of the success of NRQCD, the role of the CO mechanism is not well established yet, particularly in the J/ψ production case. The substantial theoretical progress in the next-to-leading-order (NLO) calculations shows that there is not a convincing mechanism to explain the J/ψ production data in various experiments self-consistently yet. For $J/\psi + c\bar{c} + X$ [2] and $J/\psi + X_{\text{non-}c\bar{c}}$ [3] production in e^+e^- annihilation at B -factories, the CS processes themselves can account for the cross sections when the NLO QCD corrections [4–7] and relativistic corrections [8,9] are taken into account, which leaves very little room for the CO contribution [10]. For J/ψ production from Z decay, after including the NLO QCD correction, the CS result [11] just gives one-half of the experimental measurement and the other-half might be explained by the CO contribution. The transverse momentum (p_t) distribution and the polarization parameters of J/ψ photoproduction at HERA can not be well described by the CS channel [12,13] at QCD NLO, it seems that the p_t distribution of J/ψ photoproduction can be explained by the CO and CS

contribution together at QCD NLO [14]. For J/ψ hadroproduction, together with the CS contribution [15–17] and the CO contribution [18,19] at NLO in α_s , we cannot describe the Tevatron results about the p_t distribution of the J/ψ cross section and polarization simultaneously yet.

In order to clarify such a puzzling theoretical situation, it is worth further investigation of some other J/ψ production processes, one of which is the inclusive J/ψ production in Υ decay. From the theoretical point of view, because Υ predominately decays into three gluons via $b\bar{b}$ annihilation, it is proposed [20,21] that in the rich-gluon final-state environment, abundant J/ψ can be produced through the $c\bar{c}$ pair in a $\text{CO } ^3S_1$ configuration. Hence, the inclusive J/ψ production in Υ decay will be another good probe to discriminate the CS and CO mechanism. The present CO prediction of the branching ratio is $\mathcal{B}(\Upsilon \rightarrow J/\psi + X) = 6.2 \times 10^{-4}$ [20,21] with about 10% feed-down contribution from $\psi(2S)$ and 10% from χ_{cJ} [22]. While the correct CS result, which was overestimated by about 1 order of magnitude before [23,24], is only 4.2×10^{-5} [25]. On the experimental side, the branching ratio for $\Upsilon \rightarrow J/\psi + X$ have been measured by a few collaborations about 20 years ago [26–28], and recently, a more precise measurement carried by the CLEO Collaboration gave [29]

$$\mathcal{B}(\Upsilon \rightarrow J/\psi + X) = (6.4 \pm 0.4 \pm 0.6) \times 10^{-4}. \quad (1)$$

It can be seen that the CLEO result is in good agreement with the CO prediction, but the J/ψ momentum distribution measured by CLEO [29] is much softer than the CO prediction [20,21]. In a very recent work [30], it is found that the momentum spectrum can be significantly softened after combining the NRQCD and soft collinear effective theory (SCET) in the kinematic endpoint region. However, it yields a much smaller branching ratio. This may indicate that the CO processes do not contribute dominantly.

In the CS case, the result at QCD and QED leading-order (LO) [25] is about an order of magnitude smaller than the experimental result. To investigate the CS contribution for the J/ψ production in Y decay more precisely, in this work, we consider the $\mathcal{O}(\alpha_s^6)$ contributions from the $Y \rightarrow J/\psi + gg$ and $Y \rightarrow J/\psi + gggg$ processes. It was mentioned in Ref. [22] that these two processes had been crudely estimated and the branching ratio is a few of 10^{-4} , which is comparable to the CLEO data. Since the former calculation is rough and without any publication and detail, it is necessary to give an exact result and a complete analysis of these two processes. To perform the calculations, we employ the Feynman diagram calculation (FDC) package [31].

According to the NRQCD factorization approach, at the leading-order of v_b^2 and v_c^2 , the CS contribution to $Y \rightarrow J/\psi + X$ is expressed as:

$$d\Gamma(Y \rightarrow J/\psi + X) = d\hat{\Gamma}(b\bar{b}[\bar{^3S_1}, \underline{1}] \rightarrow c\bar{c}[\bar{^3S_1}, \underline{1}] + X) \times \langle Y | \mathcal{O}_1(^3S_1) | Y \rangle \langle \mathcal{O}_1^\psi(^3S_1) \rangle, \quad (2)$$

where $d\hat{\Gamma}$ is partonic partial decay width which can be calculated perturbatively. By dimensional analysis, it is easy to derive that the general expression of the partial width is written as

$$\hat{\Gamma} = \frac{1}{3(2N_c)^2} \frac{\alpha_s^6}{m_b^5} f(r) \quad (3)$$

where $r = m_c/m_b$ is a dimensionless parameter and f is a process dependent function of r . The $\langle Y | \mathcal{O}_1(^3S_1) | Y \rangle$ and $\langle \mathcal{O}_1^\psi(^3S_1) \rangle$ in Eq. (2) are the nonperturbative matrix elements, which will be determined phenomenologically. To be consistent with our former work [25], we keep the factor $\frac{1}{3(2N_c)^2}$ explicitly.

The $\mathcal{O}(\alpha_s^6)$ $Y \rightarrow J/\psi + gg$ process has 36 one-loop Feynman diagrams at leading-order. To simplify the calculation, the diagrams which are related by reversing the direction of the b -quark or c -quark line in the fermion loop

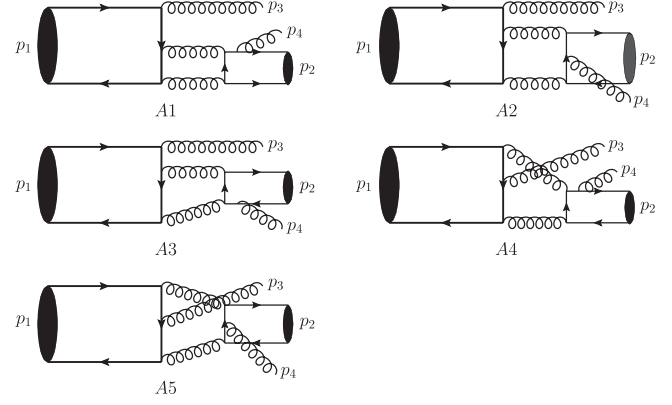


FIG. 1. The typical Feynman diagrams of five of ten groups in the CS $Y \rightarrow J/\psi + gg$ process. The other five typical ones can be obtained by exchanging the positions of the two final-state gluons.

are put together. Then they are divided into ten groups, the representative ones are shown in Fig. 1, and the others can be obtained by exchanging the positions of the two final-state gluons. For diagrams in the same group, their amplitudes are equal to each other when ignoring the color factor, thus only the $d^{abc}d^{abc}$ piece in the color factor will survive after all the diagrams are summed up in each group. It is found that there are infrared divergences in the amplitudes of diagrams in A1, A2, A4, A5 groups, at least in Feynman gauge. And the divergence terms in A1(A2) groups cancel those in A4(A5), then the total amplitude is finite. The amplitude of each diagram in group A3 is finite individually because in these diagrams there is no such virtual gluon which joins two on-shell (anti)quarks or one on-shell quark and one on-shell antiquark.

Before showing the result, we would like to address some nontrivial techniques treated in the calculation. By applying the FDC package, the general expression of the Feynman amplitude for $Y(p_1, \epsilon_1) \rightarrow J/\psi(p_2, \epsilon_2) + g(p_3, \epsilon_3) + g(p_4, \epsilon_4)$ process is generated as:

$$\begin{aligned} M = & \epsilon_1 \cdot \epsilon_2 \epsilon_3 \cdot \epsilon_4 c_{41} + \epsilon_1 \cdot \epsilon_3 \epsilon_2 \cdot \epsilon_4 c_{42} + \epsilon_1 \cdot \epsilon_4 \epsilon_2 \cdot \epsilon_3 c_{43} + p_4 \cdot \epsilon_2 p_4 \cdot \epsilon_3 \epsilon_1 \cdot \epsilon_4 c_{19} + p_4 \cdot \epsilon_1 (p_4 \cdot \epsilon_2 \epsilon_3 \cdot \epsilon_4 c_{37} \\ & + p_4 \cdot \epsilon_3 \epsilon_2 \cdot \epsilon_4 c_{39}) + p_3 \cdot \epsilon_4 [p_4 \cdot \epsilon_1 (\epsilon_2 \cdot \epsilon_3 c_{21} + p_4 \cdot \epsilon_2 p_4 \cdot \epsilon_3 c_9) + p_4 \cdot \epsilon_2 \epsilon_1 \cdot \epsilon_3 c_{29} + p_4 \cdot \epsilon_3 \epsilon_1 \cdot \epsilon_2 c_{31}] \\ & + p_3 \cdot \epsilon_2 [p_4 \cdot \epsilon_3 \epsilon_1 \cdot \epsilon_4 c_{20} + p_4 \cdot \epsilon_1 \epsilon_3 \cdot \epsilon_4 c_{35} + p_3 \cdot \epsilon_4 (\epsilon_1 \cdot \epsilon_3 c_{27} + p_4 \cdot \epsilon_1 p_4 \cdot \epsilon_3 c_{10})] + p_3 \cdot \epsilon_1 [p_4 \cdot \epsilon_2 \epsilon_3 \cdot \epsilon_4 c_{38} \\ & + p_4 \cdot \epsilon_3 \epsilon_2 \cdot \epsilon_4 c_{40} + p_3 \cdot \epsilon_4 (\epsilon_2 \cdot \epsilon_3 c_{22} + p_4 \cdot \epsilon_2 p_4 \cdot \epsilon_3 c_{11}) + p_3 \cdot \epsilon_2 (\epsilon_3 \cdot \epsilon_4 c_{36} + p_3 \cdot \epsilon_4 p_4 \cdot \epsilon_3 c_{12})] \\ & + p_2 \cdot \epsilon_3 \{ p_4 \cdot \epsilon_2 \epsilon_1 \cdot \epsilon_4 c_{17} + p_4 \cdot \epsilon_1 \epsilon_2 \cdot \epsilon_4 c_{33} + p_2 \cdot \epsilon_4 [\epsilon_1 \cdot \epsilon_2 c_{26} + p_3 \cdot \epsilon_2 p_4 \cdot \epsilon_1 c_6 + p_3 \cdot \epsilon_1 (p_3 \cdot \epsilon_2 c_8 \\ & + p_4 \cdot \epsilon_2 c_7) + p_4 \cdot \epsilon_1 p_4 \cdot \epsilon_2 c_5] + p_3 \cdot \epsilon_4 (\epsilon_1 \cdot \epsilon_2 c_{25} + p_4 \cdot \epsilon_1 p_4 \cdot \epsilon_2 c_1) + p_3 \cdot \epsilon_2 (\epsilon_1 \cdot \epsilon_4 c_{18} + p_3 \cdot \epsilon_4 p_4 \cdot \epsilon_1 c_2) \\ & + p_3 \cdot \epsilon_1 (\epsilon_2 \cdot \epsilon_4 c_{34} + p_3 \cdot \epsilon_4 p_4 \cdot \epsilon_2 c_3 + p_3 \cdot \epsilon_2 p_3 \cdot \epsilon_4 c_4) \} + p_2 \cdot \epsilon_4 [p_3 \cdot \epsilon_2 (\epsilon_1 \cdot \epsilon_3 c_{28} + p_4 \cdot \epsilon_1 p_4 \cdot \epsilon_3 c_{14}) \\ & + p_3 \cdot \epsilon_1 (\epsilon_2 \cdot \epsilon_3 c_{24} + p_3 \cdot \epsilon_2 p_4 \cdot \epsilon_3 c_{16} + p_4 \cdot \epsilon_2 p_4 \cdot \epsilon_3 c_{15}) + p_4 \cdot \epsilon_1 (\epsilon_2 \cdot \epsilon_3 c_{23} + p_4 \cdot \epsilon_2 p_4 \cdot \epsilon_3 c_{13}) \\ & + p_4 \cdot \epsilon_2 \epsilon_1 \cdot \epsilon_3 c_{30} + p_4 \cdot \epsilon_3 \epsilon_1 \cdot \epsilon_2 c_{32}] \end{aligned} \quad (4)$$

where c_i , $i = 1, \dots, 43$ are the coefficients of the Lorentz structure and all the loop diagrams contribute to them. From the general expression in Eq. (4), it is easy to understand why the tensor reduction procedures are very complicated and will generate complicated results for the coefficients c_i .

These complicated results of c_i may contain fake pole structures and cause big number cancellation problems, and finally will spoil numerical calculation in limited precision cases. In fact, it really took place in our numerical calculation. We found it is impossible to control the cancellation of the big numbers and to obtain correct results in double precision FORTRAN calculations. In quadruple precision FORTRAN calculations, we can obtain the correct results by introducing cut-conditions to control these fake poles in phase space integration. To demonstrate that our treatment is suitable, we define a cut condition parameter in phase space integration as

$$A = \frac{\Gamma(|M|^2 = 1, \text{ with cuts})}{\Gamma(|M|^2 = 1, \text{ without cuts})} \quad (5)$$

and calculate the partial decay width numerically with different cut condition parameter. The results are:

$$\begin{aligned} \Gamma &= a(1.440 \pm 0.001) \times 10^{-10} \quad \text{for } A = 1 - 0.04, \\ \Gamma &= a(1.446 \pm 0.001) \times 10^{-10} \quad \text{for } A = 1 - 0.005, \\ \Gamma &= a(1.450 \pm 0.001) \times 10^{-10} \quad \text{for } A = 1 - 0.0005, \end{aligned} \quad (6)$$

where all the calculations are under control in quadruple precision FORTRAN calculations, and a is just a constant. We have tried to do the calculation with $A = 1 - 0.00005$ and found a divergent result. This means that the big number cancellation will be out of control even in quadruple precision FORTRAN when A is very close to 1. Therefore, our following calculations for $Y \rightarrow J/\psi + gg$ are based on the cut condition parameter $A = 1 - 0.0005$. Moreover, to check the gauge invariance, in the expression of Eq. (4) we replace the gluon polarization vector ϵ_3 (or ϵ_4) by its 4-momentum p_3 (or p_4) in the final numerical calculation. Apparently, the result should be zero and our result reproduces it.

Now, we proceed to present our results. Since the two interior gluons can be on-shell simultaneously in this process, the amplitude will be complex-valued. And we use the superscript ‘Im’ to denote the contribution of the real process $Y \rightarrow 3g$ followed by $gg \rightarrow J/\psi + g$. Setting $m_c = m_{J/\psi}/2 = 1.548$ GeV and $m_b = m_Y/2 = 4.73$ GeV, which corresponds to $r = 1.548/4.73 = 0.327$, we get $f_{gg}(r) = 2.07$ and $f_{gg}^{\text{Im}}(r) = 0.741$ which is about 1/3 of the total result. To show the dependence of f on r , we also list some of the numerical results of $f(r)$ in Table I, where r is in the range of $0.275 < r < 0.381$, which is obtained by fixing the value of m_b and varying m_c from 1.3 GeV to 1.8 GeV [23]. For comparison, we also list the results of $f_{ccg}(r)$ for the $\mathcal{O}(\alpha_s^5)$ $Y \rightarrow J/\psi + c\bar{c} + g$

TABLE I. The values of $f(r)$ for $J/\psi + c\bar{c} + g$ (f_{ccg}), $J/\psi + gg$ (f_{gg} and f_{gg}^{Im}), $J/\psi + gggg$ (f_{4g}) production in Y decay with different inputs of $r = \frac{m_c}{m_b}$.

r	$f_{ccg}(r)$	$f_{gg}(r)$	$f_{gg}^{\text{Im}}(r)$	$f_{4g}(r)$
0.275	0.904	2.94	1.02	1.35×10^{-2}
0.296	0.567	2.54	0.892	1.08×10^{-2}
0.317	0.345	2.21	0.786	0.880×10^{-2}
0.327	0.269	2.07	0.741	0.800×10^{-2}
0.338	0.202	1.94	0.696	0.721×10^{-2}
0.361	0.105	1.68	0.612	0.585×10^{-2}
0.381	0.055	1.49	0.547	0.490×10^{-2}

process. It can be seen that both the value of $f_{gg}(r)$ and that of $f_{gg}^{\text{Im}}(r)$ do not change sharply, when r goes from 0.275 to 0.381, and this behavior is quite different from what happens to $f_{ccg}(r)$. Also the ratio of $f_{gg}^{\text{Im}}(r)$ to $f_{gg}(r)$ changes very little with r .

There are 216 Feynman diagrams in the CS $Y \rightarrow J/\psi + gggg$ process, and the typical one is shown in Fig. 2. It is a tree process without infrared divergence, and the numerical results are calculated straightforwardly with the help of FDC package. When $r = 0.327$, we get $f_{4g}(r) = 0.8 \times 10^{-2}$, which is more than two orders less than $f_{gg}(0.327)$. Some other numerical results of $f_{4g}(r)$ for $0.275 < r < 0.381$ are also listed in Table I. Like $f_{gg}(r)$, the function $f_{4g}(r)$ also does not depend on r seriously, but its value is too small compared to the values of the f functions of the other processes. One possible reason is that the five-body phase space is much smaller than the three-body phase space.

Besides $f_{gg}(r)(f_{4g}(r))$, the partial decay width $\Gamma(Y \rightarrow J/\psi + gg(4g))$ also depends on the choice of the values of the two NRQCD long-distance matrix elements, the coupling constant α_s and the b quark mass m_b . The value of $\langle \mathcal{O}_1^\psi(^3S_1) \rangle \simeq 3 \langle J/\psi | \mathcal{O}(^3S_1) | J/\psi \rangle$ can be extracted from J/ψ decay into e^+e^- by using up to the α_s order result

$$\Gamma(J/\psi \rightarrow e^+e^-) = \frac{2\pi e_c^2 \alpha^2}{3m_c^2} \left(1 - \frac{16\alpha_s}{3\pi} \right) \langle \psi | \mathcal{O}_1(^3S_1) | \psi \rangle. \quad (7)$$

Using $\alpha = 1/128$, $m_c = 1.548$ GeV, $\alpha_s(2m_c) = 0.26$, $\Gamma(J/\psi \rightarrow e^+e^-) = 5.54$ keV [32], we get $\langle \mathcal{O}_1^\psi(^3S_1) \rangle = 1.25$ GeV³. And $\langle Y | \mathcal{O}(^3S_1) | Y \rangle = 2.92$ GeV³ is determined in a similar way with $m_b = 4.73$ GeV, $\alpha_s(2m_b) = 0.18$,

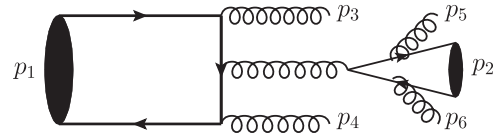


FIG. 2. One of the 216 Feynman diagrams for the CS $Y \rightarrow J/\psi + gggg$ process.

$\Gamma(Y \rightarrow e^+ e^-) = 1.29 \text{ keV}$ [32]. The uncertainty from the choice of the renormalization scale is quite large since there are two typical energy scales m_b and m_c in the calculation. By choosing $\mu = 2m_c$, we find

$$\begin{aligned}\Gamma^g &= \Gamma(Y \rightarrow J/\psi + gg) + \Gamma(Y \rightarrow J/\psi + 4g) \\ &= 9.1 \times 10^{-3} \text{ keV}\end{aligned}\quad (8)$$

It corresponds to

$$\begin{aligned}\mathcal{B}^g &= \mathcal{B}(Y \rightarrow J/\psi + gg) + \mathcal{B}(Y \rightarrow J/\psi + 4g) \\ &= 1.7 \times 10^{-4}\end{aligned}\quad (9)$$

which is coincident with the rough result mentioned in Ref. [22]. However, the branching ratio becomes much smaller and is only 2.32×10^{-5} when choosing $\mu = 2m_b$. This is because the processes are at α_s^6 order. Note that, seemingly, the branching ratio also strongly depends on m_b as m_b^{-5} , but in fact the dependence is m_b^{-3} because of the dependence of the nonperturbative matrix element $\langle Y | \mathcal{O}(\mathcal{S}_1) | Y \rangle$ on m_b from its phenomenological determination. To obtain the above numerical results for the branching ratio, the experimental measurement of the Y total decay width $\Gamma_Y = 53 \text{ keV}$ [32] is used.

Since the J/ψ is produced through the three-gluon decay channel of Y in these two processes, it is natural to normalize the partial width to the decay width of $Y \rightarrow ggg$, which at LO in α_s is given by

$$\Gamma(Y \rightarrow ggg) = \frac{20\alpha_s^3}{243m_b^2}(\pi^2 - 9)\langle Y | \mathcal{O}(\mathcal{S}_1) | Y \rangle. \quad (10)$$

Then the branching ratio is expressed in an alternate form

$$\mathcal{B}^g = \Gamma_{\text{Nor}}^g \times \mathcal{B}(Y \rightarrow ggg), \quad (11)$$

where

$$\Gamma_{\text{Nor}}^g = \frac{81(f_{gg}(r) + f_{4g}(r))\alpha_s^3\langle \mathcal{O}_1^\psi(\mathcal{S}_1) \rangle}{20(2N_c)^2m_b^3(\pi^2 - 9)}, \quad (12)$$

and $\mathcal{B}(Y \rightarrow ggg) = 84\%$ is obtained by assuming $\mathcal{B}(Y \rightarrow ggg) \approx \mathcal{B}(Y \rightarrow \text{light hadron(LH)})^1$ [32]. To calculate the branching ratio in this way is equivalent to determining $\alpha_s^3\langle Y | \mathcal{O}(\mathcal{S}_1) | Y \rangle$ from light hadron decay of Y and can reduce the uncertainty from α_s . Our following results are all calculated based on Eq. (11).

The numerical results of “ $f(r)$ ” for each decay process are presented in Table I, and it shows that the values of $f_{(gg)}(r)$ change slowly when r goes from 0.275 to 0.381. The Feynman diagrams in Fig. 1 indicate that the process $Y \rightarrow J/\psi + gg$ can be viewed as $Y \rightarrow g^{(*)}g^{(*)2}$ followed by $g^{(*)}g^{(*)} \rightarrow J/\psi + g$. Then the normalized Γ_{Nor}^g can cancel part of the contribution at the m_b scale, so similar

to what is done in Ref. [20] we choose the scale of α_s to be $2m_c$. The theoretical uncertainties of $Y \rightarrow J/\psi + gggg$ can be analyzed in the same way.

By setting the default parameter choice: $m_b = 4.73 \text{ GeV}$, $r = 0.327$, $\langle \mathcal{O}_1^\psi(\mathcal{S}_1) \rangle = 1.25 \text{ GeV}^3$ and $\alpha_s(2m_c) = 0.26$, we obtain

$$\mathcal{B}^g = \Gamma_{\text{Nor}}^g \times \mathcal{B}(Y \rightarrow ggg) = 0.47 \times 10^{-4}. \quad (13)$$

Using the same inputs to reestimate the result in Ref. [25] and adding it up with the contribution in Eq. (13), we obtain the total CS singlet prediction

$$\mathcal{B}(Y \rightarrow J/\psi + X) = 0.90 \times 10^{-4}, \quad (14)$$

where the total contribution from the $\mathcal{O}(\alpha_s^6) J/\psi + gg$ and $J/\psi + gggg$ processes is as important as those calculated in Ref. [25]. It is obvious that the uncertainties are from the b quark mass m_b , the scaleless functions $f_{gg}(r)$ and $f_{4g}(r)$, and the choice of the scale of α_s . To estimate the uncertainty, we used $m_b = 4.6 \text{ GeV}$, $r = 0.296$ and $\mu = 2m_c$ for the upper bound; $m_b = 4.9 \text{ GeV}$, $r = 0.361$ and $\mu = 2m_c$ for the lower bound, then the branching ratio is represented as:

$$\mathcal{B}(Y \rightarrow J/\psi + X) = 0.90_{-0.31}^{+0.49} \times 10^{-4}. \quad (15)$$

Furthermore the central result of the total branching ratio turns to be a much smaller value 5.2×10^{-5} (6.3×10^{-5}) by choosing the scale to be $2m_b$ ($2\sqrt{m_b m_c}$) and $\alpha_s(2m_b) = 0.18$ ($\alpha_s(2\sqrt{m_b m_c}) = 0.21$) and keeping the other parameters unchanged.

The experimental result in Eq. (1) includes the feed-down contributions of χ_{cJ} , which are $<8.2, 11, 10$ percents for $J = 0, 1, 2$, respectively, and 24% feed-down contribution of $\psi(2S)$. Removing the feed-down contributions, the branching ratio of direct J/ψ production in Y decay would be

$$\mathcal{B}(Y \rightarrow J/\psi_{\text{direct}} + X) = 3.52 \times 10^{-4}. \quad (16)$$

which is about 3.8 times larger than the current CS prediction.

For the J/ψ momentum spectrum, the normalized decay width defined in Eq. (12) is used to present the results with default parameter choice. Both the total result (solid line) and the imaginary part contribution (dashed line) for $\mathcal{O}(\alpha_s^6) J/\psi + gg$ process are shown in Fig. 3 with very similar shape. A summarized CS contribution to the $p_{J/\psi}$ distribution of the normalized decay width is shown in Fig. 4. We find the peak of the total result curve is at $p_{J/\psi} = 2.7 \text{ GeV}$, which is a little larger than that of the CLEO measurement [29].

It is found that the J/ψ production in association with the $c\bar{c}$ pair is an important mechanism for J/ψ electroproduction [2,3] in the Belle experiment. And theoretically, the contribution of the $p\bar{p} \rightarrow J/\psi + c\bar{c} + X$ process to J/ψ hadroproduction at the Tevatron is also

¹The contribution of $Y \rightarrow \gamma^* \rightarrow q\bar{q}$ is excluded.

² $g^{(*)}$ means the gluon can either be virtual or real.

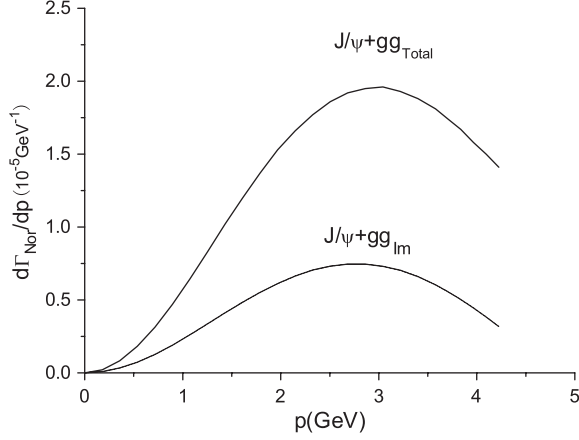


FIG. 3. The normalized partial width of the $\mathcal{O}(\alpha_s^6)$ $Y \rightarrow J/\psi + gg$ process as a function of J/ψ momentum $p_{J/\psi}$. The solid line is the total result, and the dashed line is the contribution from the imaginary part in the Feynman amplitude.

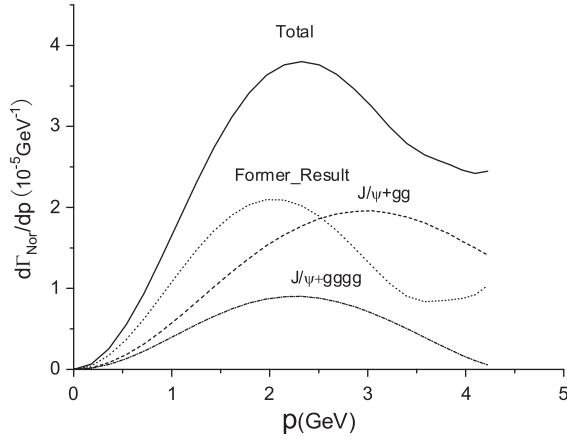


FIG. 4. The normalized partial width for the CS J/ψ production in Y decay as function of J/ψ momentum $p_{J/\psi}$. The solid line is the total result. the dashed line is the contribution of the $\mathcal{O}(\alpha_s^6)$ $Y \rightarrow J/\psi + gg$ process. The dashed-dotted line is $100 \times$ the contribution $\mathcal{O}(\alpha_s^6)$ $Y \rightarrow J/\psi + gggg$. The dotted line is the contribution calculated in Ref. [25], which includes the $\mathcal{O}(\alpha_s^5)$ $Y \rightarrow J/\psi + c\bar{c}g$ and $\mathcal{O}(\alpha^2\alpha_s^2)$ $Y \rightarrow J/\psi + gg$ and $Y \rightarrow J/\psi + c\bar{c}$ processes.

found to be nonignorable [33,34]. The ratio of J/ψ produced in association with the $c\bar{c}$ pair to J/ψ plus anything may also be a good probe to reveal the J/ψ production mechanism in Y decay and to clarify the conflict between the CLEO measurement and theoretical prediction. Choosing $\alpha_s(2m_c) = 0.259$, we give the CS prediction for the ratio R_{cc}

$$R_{cc} = \frac{\mathcal{B}(Y \rightarrow J/\psi + c\bar{c} + X)}{\mathcal{B}(Y \rightarrow J/\psi + X)} = 0.39^{+0.21}_{-0.20}, \quad (17)$$

where the center, upper and lower bound values correspond to $r = 0.327, 0.296$ and 0.361 , respectively, and the associated charmed particles process includes the $\mathcal{O}(\alpha_s^5)$ $Y \rightarrow J/\psi + c\bar{c}g$ subprocess, which is dominant, and the $\mathcal{O}(\alpha^2\alpha_s^2)$ $Y \rightarrow \gamma^* \rightarrow J/\psi + c\bar{c}$ subprocess. On the contrary, the CO prediction of R_{cc} is only at the level of 1% [20], which is quite different from the CS prediction. Unlike the branching ratio, the theoretical prediction for R_{cc} only depends on r and α_s , which results in a relatively small uncertainty. Particularly, if we drop the contribution of the QED part, R_{cc} is just proportional to α_s . In Ref. [4,5], the authors find the enhancement of the NLO QCD corrections is large in the $e^+e^- \rightarrow J/\psi + c\bar{c}$ process. It indicates that the result in Eq. (17)] is only a very preliminary result and to get a more solid prediction the contribution of the NLO QCD corrections to the $Y \rightarrow J/\psi + c\bar{c} + g$ process should be taken into account. Calculating the NLO QCD corrections to $Y \rightarrow J/\psi + c\bar{c} + g$ process is beyond the scope of this work and will not be discussed here. In the end, the J/ψ momentum spectra for the associated process and non- $c\bar{c}$ process are given in Fig. 5 for comparison.

In summary, in this work, we calculate the $\mathcal{O}(\alpha_s^6)$ CS contribution of $Y \rightarrow J/\psi + gg$ and $Y \rightarrow J/\psi + gggg$ processes to the inclusive J/ψ production in Y decay. The branching ratio is estimated in two ways. In the first way, the numerical results of partial width and branching ratios are all evaluated directly. We also find the result is closer to the experimental data when the values of the parameters are properly chosen, which is also coincident with the roughly estimated result mentioned in Ref. [22]. However, the uncertainty of this way is very large and the branching ratio can be in a wide range of $2.3 \times 10^{-5} \sim 1.7 \times 10^{-4}$. In the second way, the branching ratio is calculated by using the normalized decay width, which seems more reliable. After combining the present result with the contribution calculated in our previous work [25],

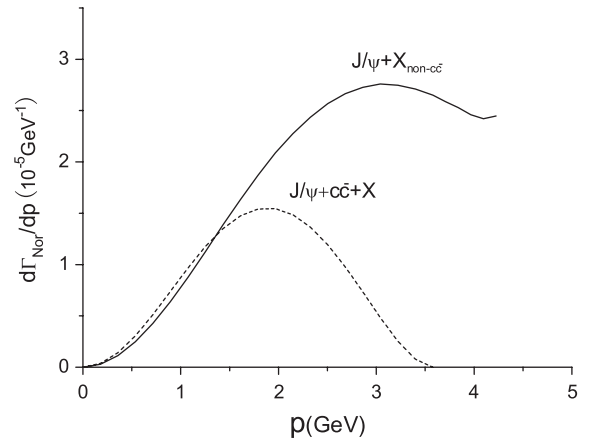


FIG. 5. The normalized partial width of Y decay into $J/\psi + c\bar{c} + X$ process as a function of J/ψ momentum $p_{J/\psi}$ (dashed line) and that for $J/\psi + X_{\text{non-}c\bar{c}}$ production (solid line).

we find now the total CS prediction is about 0.92×10^{-4} , which is still about 3.8 times less than the experimental value 3.2×10^{-4} for direct J/ψ production given by the CLEO Collaboration [29]. We also calculate the J/ψ momentum spectrum and find the peak of the color-singlet curve is close to that of the CLEO result, although being a little larger. Besides the branching ratio and the J/ψ spectrum, we also study the ratio $R_{cc} = \mathcal{B}(Y \rightarrow J/\psi + c\bar{c} + X)/\mathcal{B}(Y \rightarrow J/\psi + X)$, and find the CS prediction is much larger than that of the CO. Since the associated charmed meson process can be measured directly, an analysis of the ratio is suggested to be performed in the CLEO, Babar or Belle experiments. Now, there is still a large discrepancy between the CLEO results and NRQCD predictions. There are two points to be addressed: first, the

J/ψ production mechanism is not well understood yet, and the existence of the CO mechanism is still under debate; second the NLO QCD corrections are not included completely. Therefore, to understand the J/ψ production mechanism in Y decay and moreover in $p\bar{p}$ collisions at the Tevatron, further theoretical and experimental work are absolutely necessary.

This work is supported by the National Natural Science Foundation of China (No. 10979056 and No. 10935012), and by the Chinese Academy of Science under Project No. INFO-115-B01. The work of Zhi-guo He is partially supported by the CPAN08-PD14 contract of the CSD2007-00042 Consolider-Ingenio 2010 program, and by the FPA2007-66665-C02-01/ project (Spain).

-
- [1] G. T. Bodwin, E. Braaten, and G. P. Lepage, *Phys. Rev. D* **51**, 1125 (1995); **55**, 5853(E) (1997).
 - [2] K. Abe *et al.* (Belle Collaboration), *Phys. Rev. Lett.* **89**, 142001 (2002).
 - [3] P. Pakhlov *et al.* (Belle Collaboration), *Phys. Rev. D* **79**, 071101 (2009).
 - [4] Y. J. Zhang, Y. j. Gao, and K. T. Chao, *Phys. Rev. Lett.* **96**, 092001 (2006).
 - [5] B. Gong and J. X. Wang, *Phys. Rev. D* **80**, 054015 (2009).
 - [6] Y. Q. Ma, Y. J. Zhang, and K. T. Chao, *Phys. Rev. Lett.* **102**, 162002 (2009).
 - [7] B. Gong and J. X. Wang, *Phys. Rev. Lett.* **102**, 162003 (2009).
 - [8] Z. G. He, Y. Fan, and K. T. Chao, *Phys. Rev. D* **75**, 074011 (2007).
 - [9] Z. G. He, Y. Fan, and K. T. Chao, *Phys. Rev. D* **81**, 054036 (2010); Y. Jia, *Phys. Rev. D* **82**, 034017 (2010).
 - [10] Y. J. Zhang, Y. Q. Ma, K. Wang, and K. T. Chao, *Phys. Rev. D* **81**, 034015 (2010).
 - [11] R. Li and J. X. Wang, *Phys. Rev. D* **82**, 054006 (2010).
 - [12] P. Artoisenet, J. M. Campbell, F. Maltoni, and F. Tramontano, *Phys. Rev. Lett.* **102**, 142001 (2009).
 - [13] C. H. Chang, R. Li, and J. X. Wang, *Phys. Rev. D* **80**, 034020 (2009).
 - [14] M. Butenschoen and B. A. Kniehl, *Phys. Rev. Lett.* **104**, 072001 (2010).
 - [15] J. M. Campbell, F. Maltoni, and F. Tramontano, *Phys. Rev. Lett.* **98**, 252002 (2007).
 - [16] B. Gong and J. X. Wang, *Phys. Rev. Lett.* **100**, 232001 (2008).
 - [17] B. Gong and J. X. Wang, *Phys. Rev. D* **78**, 074011 (2008).
 - [18] E. Braaten and S. Fleming, *Phys. Rev. Lett.* **74**, 3327 (1995).
 - [19] B. Gong, X. Q. Li, and J. X. Wang, *Phys. Lett. B* **673**, 197 (2009).
 - [20] K. M. Cheung, W. Y. Keung, and T. C. Yuan, *Phys. Rev. D* **54**, 929 (1996).
 - [21] M. Napsuciale, *Phys. Rev. D* **57**, 5711 (1998).
 - [22] H. D. Trottier, *Phys. Lett. B* **320**, 145 (1994).
 - [23] S. Y. Li, Q. B. Xie, and Q. Wang, *Phys. Lett. B* **482**, 65 (2000).
 - [24] W. Han and S. Y. Li, *Phys. Rev. D* **74**, 117502 (2006).
 - [25] Z. G. He and J. X. Wang, *Phys. Rev. D* **81**, 054030 (2010).
 - [26] R. Fulton *et al.* (CLEO Collaboration), *Phys. Lett. B* **224**, 445 (1989).
 - [27] W. S. Maschmann *et al.* (Crystal Ball Collaboration), *Z. Phys. C* **46**, 555 (1990).
 - [28] H. Albrecht *et al.* (ARGUS Collaboration), *Z. Phys. C* **55**, 25 (1992).
 - [29] R. A. Briere *et al.* (CLEO Collaboration), *Phys. Rev. D* **70**, 072001 (2004).
 - [30] X. Liu, *Phys. Lett. B* **685**, 151 (2010).
 - [31] J.-X. Wang, *Nucl. Instrum. Methods Phys. Res., Sect. A* **534**, 241 (2004).
 - [32] C. Amsler *et al.* (Particle Data Group), *Phys. Lett. B* **667**, 1 (2008).
 - [33] P. Artoisenet, J. P. Lansberg, and F. Maltoni, *Phys. Lett. B* **653**, 60 (2007).
 - [34] Z. G. He, R. Li, and J. X. Wang, *Phys. Rev. D* **79**, 094003 (2009).